

Highly efficient ambient temperature photo-oxidation of CH₄ to C1 products over CeO₂ supported single-atom Fe with oxygen vacancy

Hailong Tang^a, Yongqing Ma^{a,b}, Chuhong Zhu^a, Min Wang^d, Ganhong Zheng^a,

Xiao Sun^{c,} and Meiling Wang^{a,*}*

^a School of Materials Science and Engineering, Anhui University, Hefei, 230601, China

^b Institute of Physical Science and Information Technology, Anhui University, Hefei 230601, China

^c Hefei National Laboratory for Physical Sciences at the Microscale, Key Laboratory of Surface and Interface Chemistry and Energy Catalysis of Anhui Higher Education Institutes, School of Chemistry and Materials Science, University of Science and Technology of China, Hefei 230026, China.

^d School of Physics and optoelectronics engineering, Anhui University, Hefei, 230601, China

**To whom correspondence should be addressed.*

Tel: (86) 13856996630, E-mail: mlw@ahu.edu.cn, sunxiao@ustc.edu.cn

Part S1 Characterization

Morphology of the catalysts were characterized using scanning electron microscopy (SEM, S-4800, Hitachi, Japan), transmission electron microscopy (TEM, JEOL JEM-2100, Japan) and aberration-corrected high-angle annular dark-field scanning transmission electron microscopy (AC-HAADF-STEM, Themis Z). XRD patterns were acquired on the Empyrean S3 diffractometer (Rigaku Industrial Corporation, Osaka, Japan). H nuclear magnetic resonance (HNMR) spectra were measured on a JNM-ECZ400S NMR spectrometer (Japan). XPS spectra were measured with the ESCALAB 250Xi instrument (XPS, Thermo Scientific Inc., USA). ESR spectra were measured on a EMX plus 10/12 ESR spectrometer (Bruker, Germany) in dark or under light irradiation. UV-vis DRS spectra were recorded on a U-4100 spectrometer (Shimadzu, Japan). Steady-state PL spectra were recorded at room temperature on the FLUORMAX-4P spectrofluorometers (HORIBA, France). Fourier transform infrared (FTIR) spectra were recorded on a Vertex 80 spectrometer (Bruker, Germany). Electrochemical measurements were conducted on a Zennium E electrochemical workstation (Zahner, Germany).

Part S2 DFT computational details.

The 2-layer 2×2 supercell of CeO_2 (1 1 1) slab with 96 atoms (six atomic layers) was used to build the calculation models. All the density functional theory (DFT) calculations were carried out using the Dmol³ code of Materials Studio 2019.¹ The exchange-correlation potential was calculated by the generalized gradient approximation (GGA) with the Perdew-Burke-Ernzerhof (PBE) functional.¹ The interactions between electronics and ions were described using the DFT semi-core pseudo potentials (DSPPs) core treatment, which replaces core electrons by a single effective potential and introduces some degree of relativistic correction into the core. The geometry optimization convergences tolerance was set to $0.002 \text{ Ha} \cdot \text{\AA}^{-1}$ (1 Ha = 27.2114 eV), and the total energy convergences was set to 10^{-6} Ha . The Brillouin zone was sampled with $2 \times 2 \times 1$ Monkhorst-Pack k-point mesh, and a smearing of 0.005 Ha was applied to speed up electronic convergence. Spin polarization was also applied to our calculations, and the real space cutoff radius was maintained as 5.0 \AA .^{2,3} The Ce

and O atoms in the bottom three layers were fixed, and the other atoms were fully relaxed. The thickness of the vacuum layer in multi-layer calculation models was set to 20 Å to avoid the unwanted interaction between the slab and its period images.

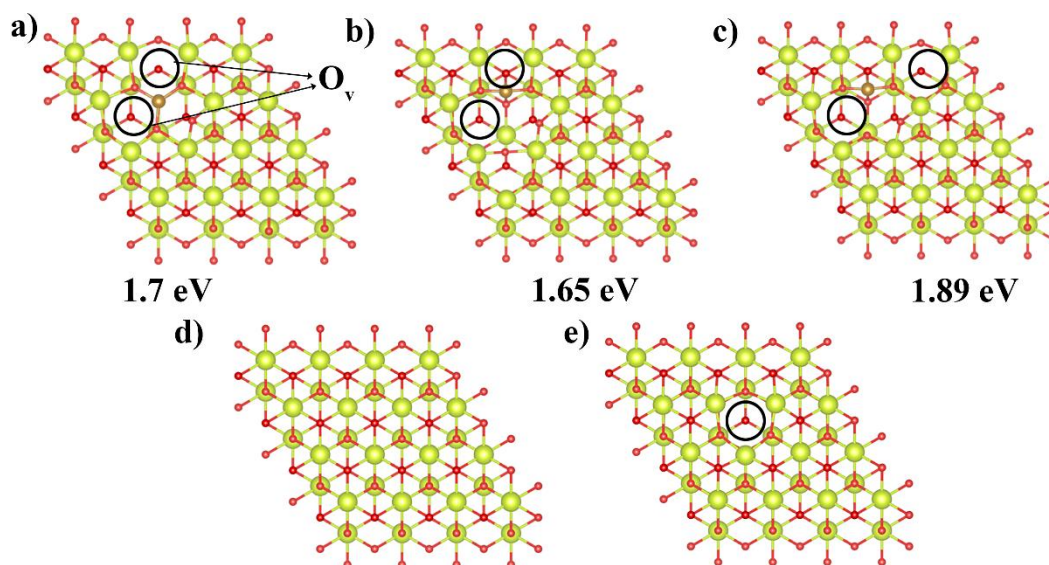


Fig. S1 a-c) Structure models of Fe-doped CeO₂ (111) with 2 O_v and their formation energy of the second O_v. Structure models of CeO₂ (111) surface d) without and e) with O_v.

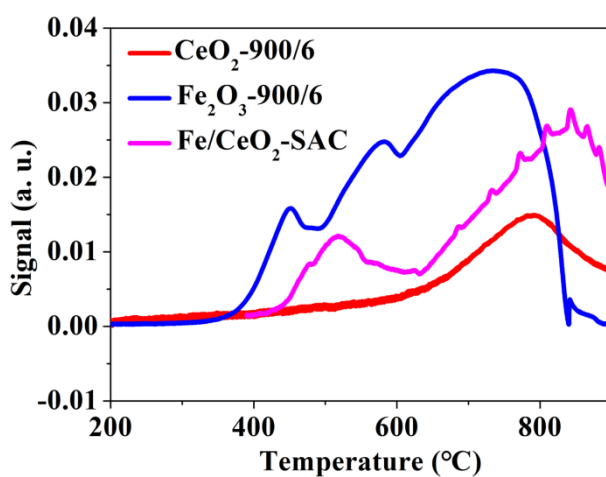


Fig. S2 H₂-TPR plots of Fe/CeO₂-900/6, Fe₂O₃-900/6 and CeO₂-900/6 respectively.

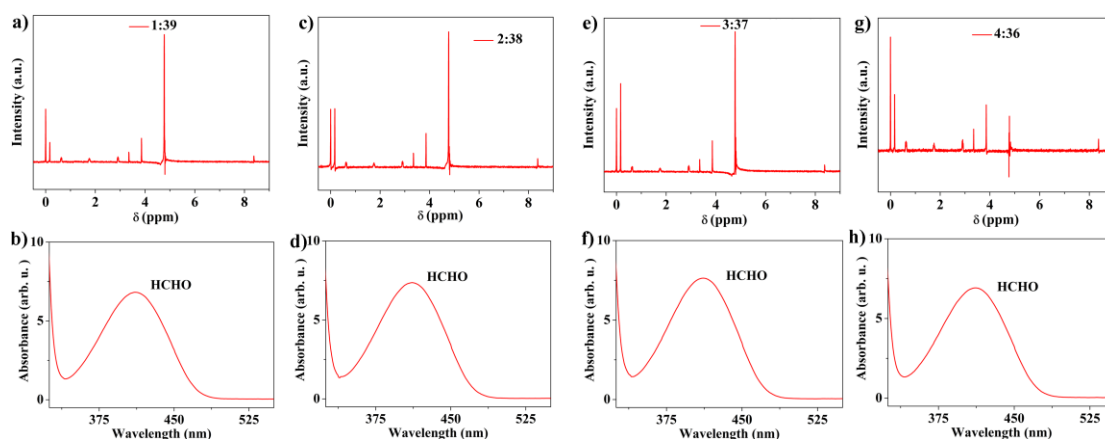


Fig. S3 HNMR and UV-vis absorption spectra of the reaction solution over catalysts with varied Fe/Ce precursor mole ratio. a, b) 1:39, c, d) 2:38, e, f) 3:37 and g, h) 4:36. Reaction conditions: CH_4 : 2 MPa, H_2O_2 : 495 μL , reaction time: 2 h, catalyst weight: 5 mg and xenon operating current: 16 A.

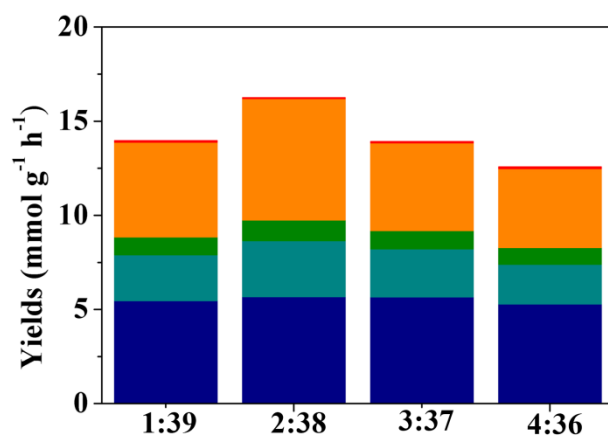


Fig. S4 The yields of C1 products over catalysts with varied Fe/Ce precursor mole ratio. Reaction conditions: CH_4 : 2 MPa, H_2O_2 : 495 μL , reaction time: 2 h, and catalyst weight: 5 mg.

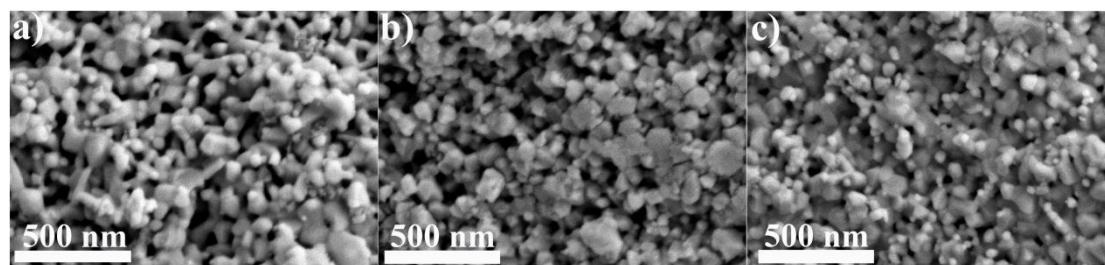


Fig. S5 SEM images of catalysts with varied Fe/Ce precursor mole ratio: a) 1:39, b) 3:37 and c) 4:36 respectively.

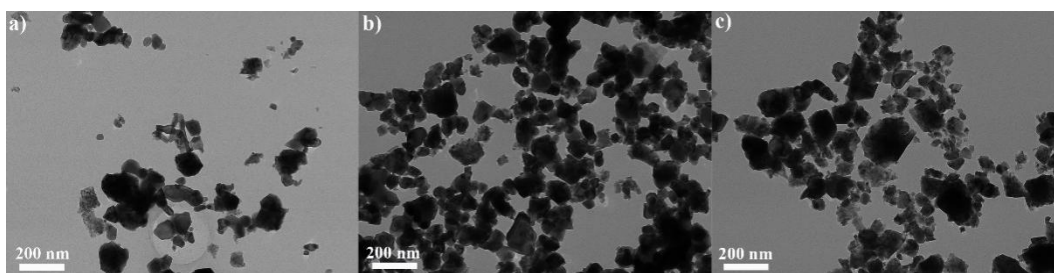


Fig. S6 TEM images of catalysts with varied Fe/Ce precursor mole ratio: a) 1:39, b) 3:37 and c) 4:36 respectively.

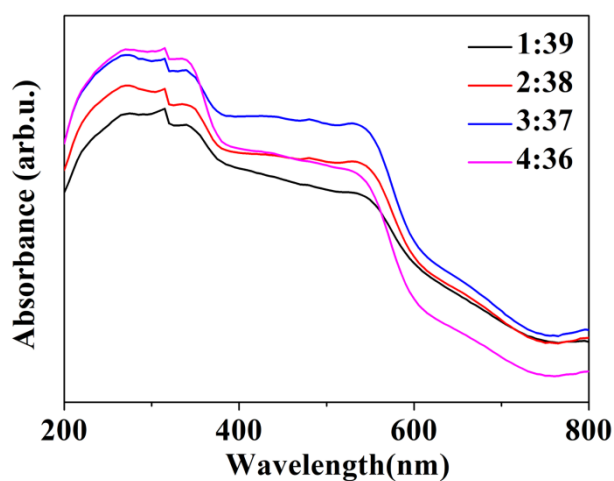


Fig. S7 UV-vis DRS spectra of varied catalysts.

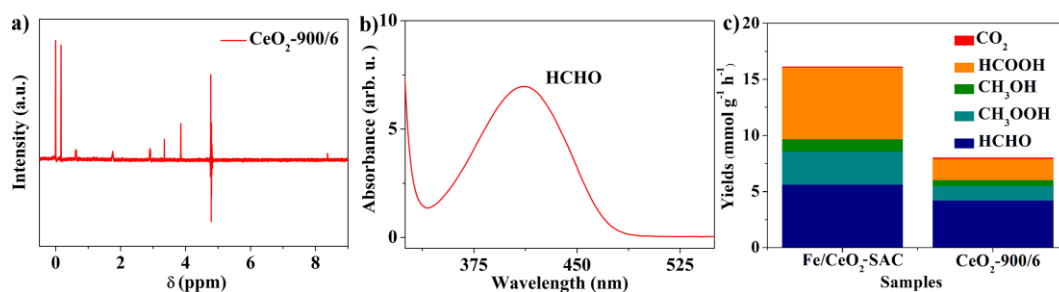


Fig. S8 a, b) ^1H NMR and UV-vis absorption spectra and c) yields of C1 products over Fe/CeO₂-SAC and CeO₂-900/6. Reaction conditions: CH₄: 2 MPa, H₂O₂: 495 μL , reaction time: 2 h, and catalyst weight: 5 mg.

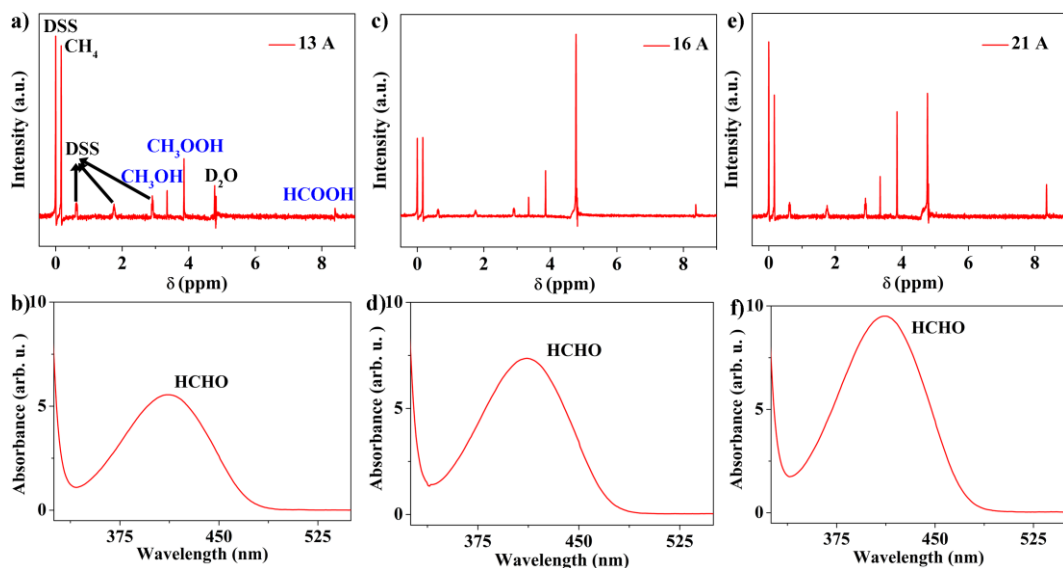


Fig. S9 HNMR and UV-vis absorption spectra of the reaction solution over Fe/CeO₂-SAC under xenon lamp operating current of a, b) 13, c, d) 16 and e, f) 21 A, respectively. Reaction conditions: CH₄: 2 MPa, H₂O₂: 495 μL, catalyst weight: 5 mg, and reaction time: 2 h.

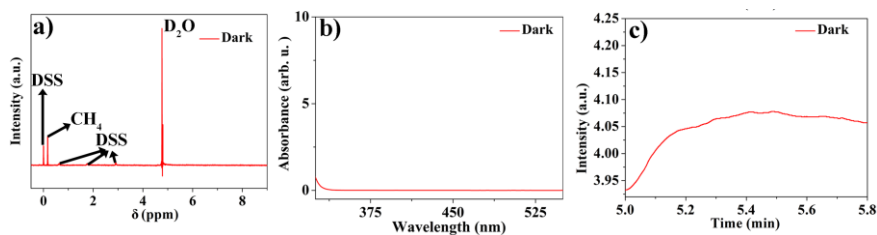


Fig. S10 a) HNMR, UV-vis and c) GC spectra of the liquid phase products over Fe/CeO₂-SAC without light illumination. Reaction conditions: CH₄: 2 MPa, H₂O₂: 495 μL, reaction time: 2 h, , catalyst weight: 5 mg, and xenon lamp operating current:

16 A.

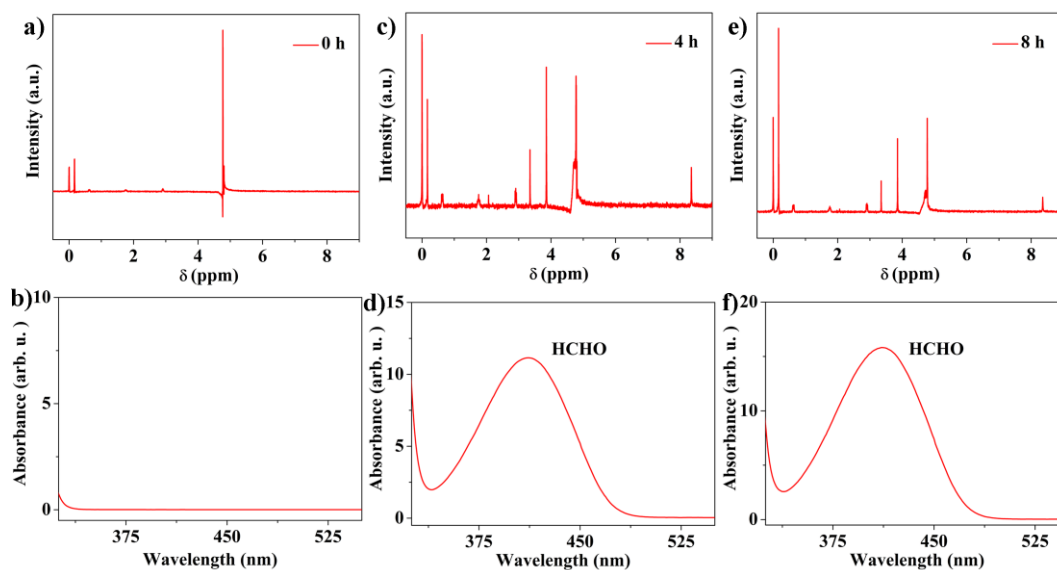


Fig. S11 HNMR and UV-vis absorption spectra of the reaction solution over Fe/CeO₂-SAC with reaction time of a, b) 0 h, c, d) 4 h and e, f) 8 h, respectively. Reaction conditions: CH₄: 2 MPa, H₂O₂: 495 μL, catalyst weight: 5 mg, and xenon lamp operating current: 16 A.

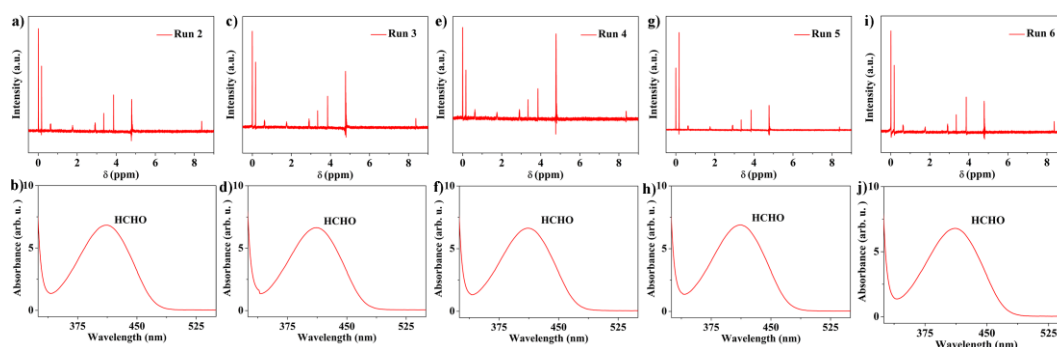


Fig. S12 HNMR and UV-vis absorption spectra of the reaction solution in the a, b) 1st, c, d) 2nd, 3rd, e, f) 4th, g, h) 5th and i, j) 6th cycle, respectively. Reaction conditions: CH₄: 2 MPa, H₂O₂: 495 μL, catalyst weight: 5 mg, reaction time: 2 h, and xenon lamp operating current: 16 A.

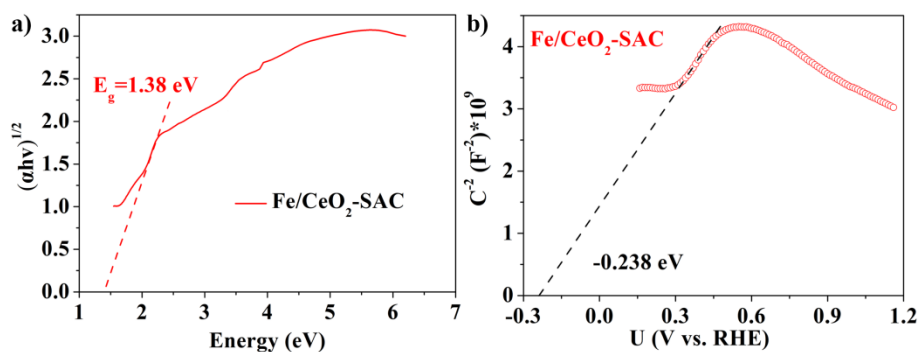


Fig. S13 a) Tauc plots and b) Mott-Schottky plots of Fe/CeO₂-SAC measured at the frequency of 1 kHz.

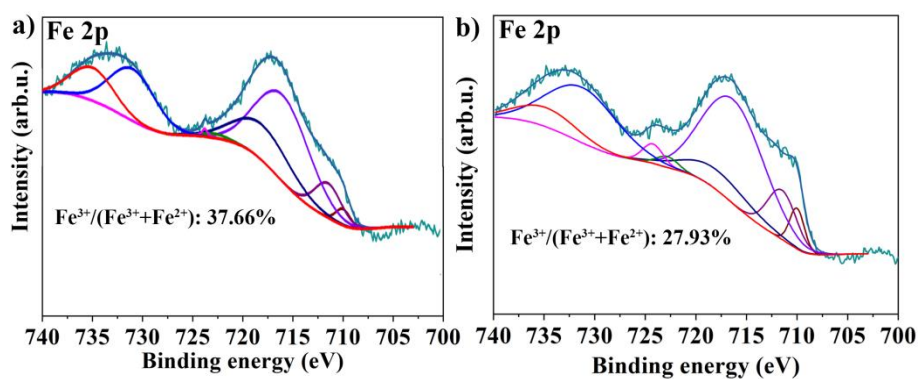


Fig. S14 Deconvoluted high-resolution Fe 2p XPS spectra a) before and b) after reaction.

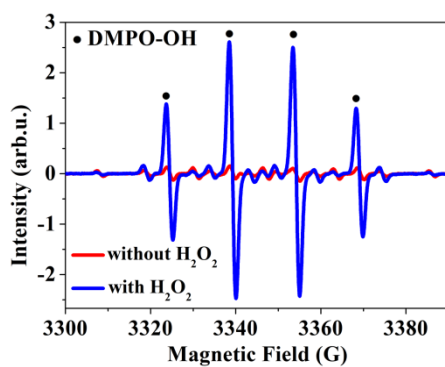


Fig. S15 ESR spectra for identifying $\cdot\text{OH}$ in H_2O solution with and without H_2O_2 respectively.

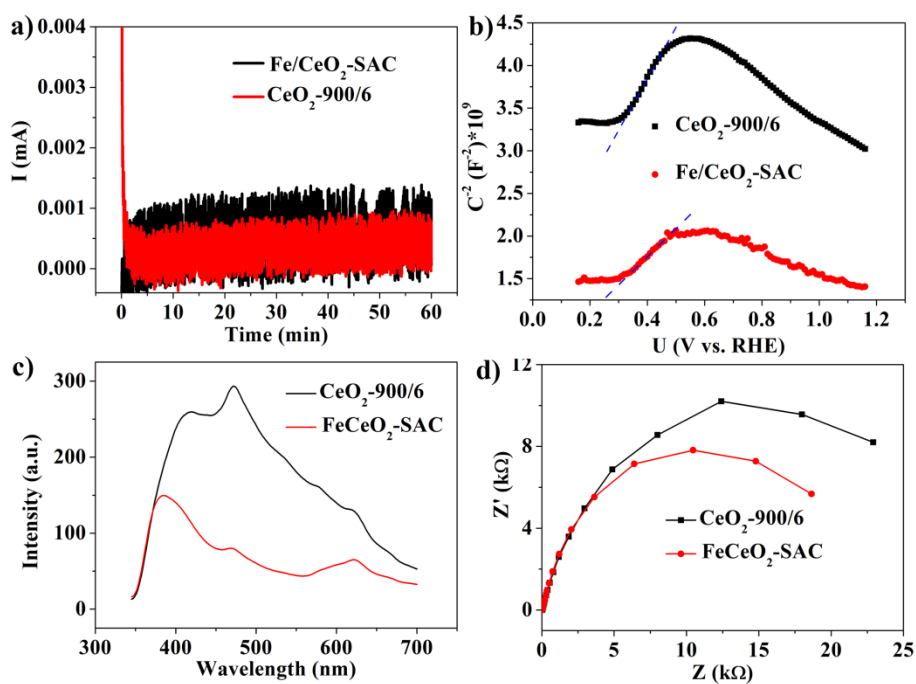


Fig. S16 a) Photocurrent curves, b) Mott–Schottky plots, c) PL spectra and d) EIS spectra of Fe/CeO₂-SAC and CeO₂-900/6.

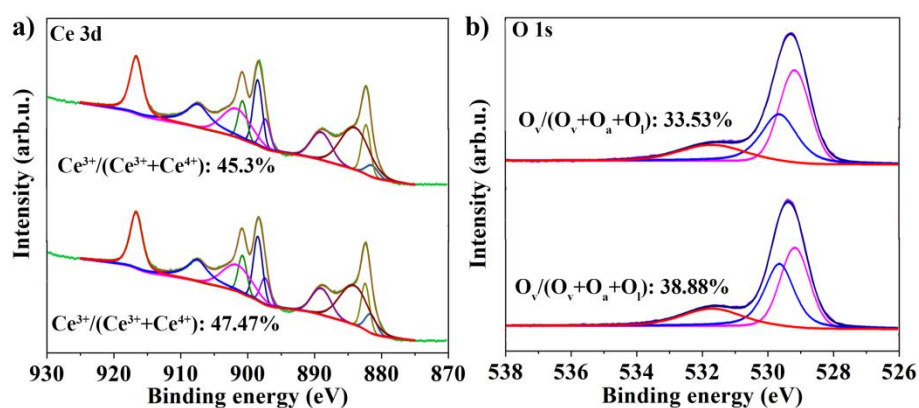


Fig. S17 Deconvoluted high-resolution a) Ce 3d and b) O 1s XPS spectra of Fe/CeO₂-SAC (down) and the referential sample prepared by calcination under air atmosphere (up).

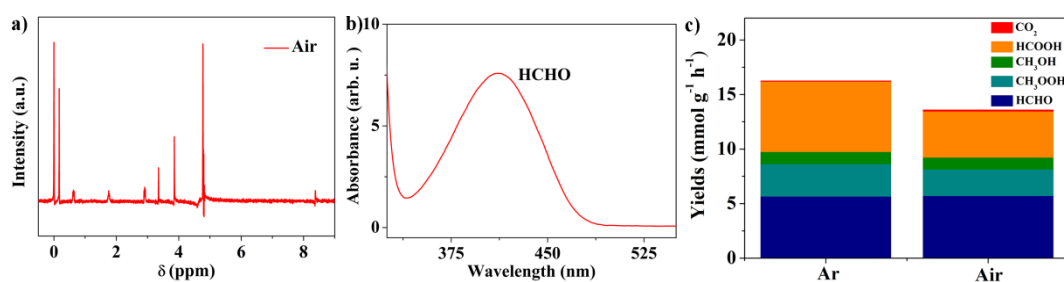


Fig. S 18 a, b) HNMR and UV-vis absorption spectra and c) yields of C1 products over Fe/CeO₂-SAC (calcinated under Ar atmosphere) and the referential sample prepared by calcination under air atmosphere. Reaction conditions: CH₄: 2 MPa, H₂O₂: 495 μL, reaction time: 2 h, and catalyst weight: 5 mg.

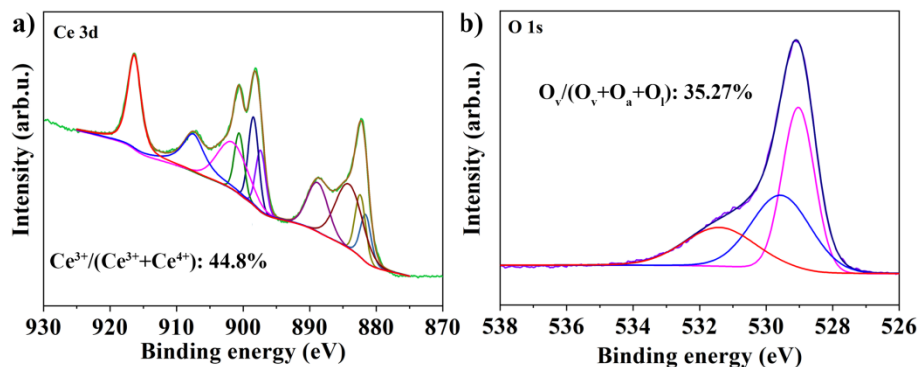


Fig. S19 Deconvoluted high-resolution a) Ce 3d and b) O 1s XPS spectra of Fe/CeO₂-SAC post-reaction.

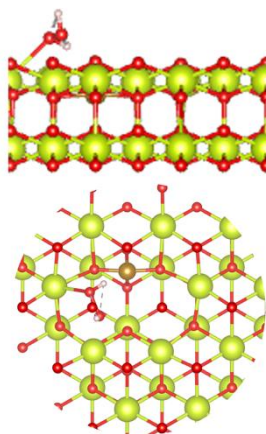


Fig. S20 Structure model of *H₂O₂.

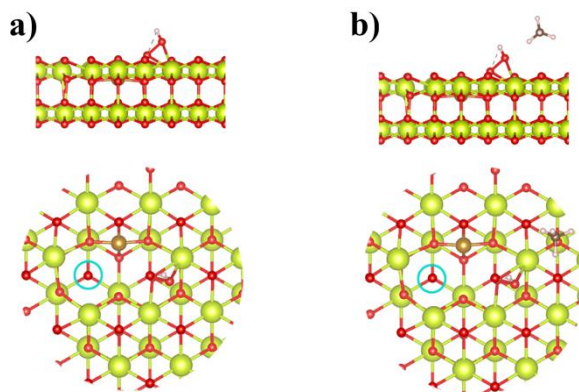


Fig. S21 Structure models of a) *OH and b) *OH+CH₄. Up: side view, down: top view.

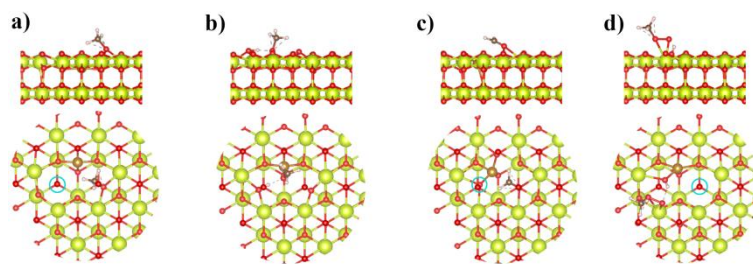


Fig. S22 Structure models of a) $*\text{CH}_3$, b) $*\text{CH}_3\text{OH}$, c) $*\text{HCHO}$ and d) $*\text{CH}_3\text{OOH}$. Up: side view, down: top view.

References

- 1 Y. Jiang, C. Lai, Q. Li, W. Gao, L. Yang, Z. Yang, R. Lin, X. Wang and X. Zhu, *Fuel*, 2020, 280, 118638.
- 2 X. Song, P. Ning, C. Wang, K. Li, L. H. Tang and X. Sun, *Appl. Surf. Sci.*, 2017, 414, 345-352.
- 3 H. Tang, T. Ju, Y. Dai, M. Wang, Y. Ma, M. Wang and G. Zheng, *J. Mater. Chem. A*, 2022, 10, 18978-18988.